Experimental Thermal and Fluid Science 72 (2016) 31–39

Contents lists available at ScienceDirect

Experimental Thermal and Fluid Science

journal homepage: www.elsevier.com/locate/etfs

Multiple vortex structures in the wake of a rectangular winglet in ground effect

Clara M. Velte [a,*], Martin O.L. Hansen [b,c], Valery L. Okulov [b,d]

[a] Department of Mechanical Engineering, Technical University of Denmark, 2800 Kgs. Lyngby, Denmark
[b] Department of Wind Energy, Technical University of Denmark, 2800 Kgs. Lyngby, Denmark
[c] Centre for Ships and Ocean Structures, Norwegian University of Science and Technology, 7491 Trondheim, Norway
[d] Institute of Thermophysics, Siberian Branch of the Russian Academy of Sciences, 630090 Novosibirsk, Russia

ARTICLE INFO

Article history:
Received 14 August 2015
Received in revised form 22 October 2015
Accepted 23 October 2015
Available online 11 November 2015

Keywords:
Vortex generator
Turbulent boundary layer flow control
Flow topology behind vortex generator
Secondary vortex structures
Vortex generator modeling
PIV reflection reduction

ABSTRACT

Patterns of vorticity in the wake of a single rectangular winglet (vortex generator) embedded in a turbulent boundary layer have been studied using Stereoscopic Particle Image Velocimetry (SPIV). The winglet was mounted normally to a flat surface with an angle to the oncoming flow. A parametric study varying the winglet height (constant aspect ratio) and angle has shown, contrary to the common classical single tip-vortex conception, that the wake generally consists of a complex system of multiple vortex structures. The primary vortex has previously been discovered to contain a direct coupling between the axial and the rotational flow. In the current work, even the longitudinal secondary structures detected from measured streamwise vorticity display similar behavior. A regime map depicting the observed stable far wake states of the multiple vortices as a function of winglet height and angle reveals complex patterns of the flow topologies not only with the primary tip vortex, but with the additional secondary structures as well. A bifurcation diagram shows distinct regimes of the various secondary structures as well as how the primary vortex is in some cases significantly affected by their presence. These data should serve as inspiration in the process of generating longitudinal vortices for enhancement of heat and mass transfer in industrial devices since the multiple vortex regimes can help improve the conditions for these exchanges. Further, these results point to a weakness in existing inviscid models not accounting for the possibility of multiple vortical structures in the wake.

1. Introduction

Vortex generators were described by Taylor as early as in the late 1940s [1–4] and have for many years been used to, e.g., delay separation and enhance mixing of momentum and heat. A common strategy to increase the heat transfer coefficient is to generate longitudinal vortices in flows whose rotating motion induces an increasing exchange of hot and cold fluid, see, e.g., [5–10]. Min and co-workers [11] have observed that the topology and composition of the longitudinal vortices can be of uttermost importance to heat transfer enhancement. Previous research has put a great deal of effort into trying to understand and optimize the effect of the devices without succeeding in finding a general approach valid independently of test bed. Except for the comprehensive combined theoretical and experimental summary of Pearcey [12], most early studies use surface visualizations and measurement techniques providing integral measures (e.g., integral forces and observation of reversed flow) in specific applications rather than seeking understanding in the detailed flow physics and characteristics. The work of Lin and co-workers presents many generic experimental studies on VGs for separation control [13–17]. One of their many findings is that for turbulent boundary layers, the smaller micro-vortex generators work very well in turbulent boundary layers even if their height is only a fraction of the boundary layer height. Their high efficiency is, from actual measurement results, explained by the much fuller velocity profile of a turbulent boundary layer as compared to a laminar one and are also hypothesized to function in themselves like 'turbulators' rather than like the classical picture of a single wing tip vortex provided by Taylor [1–4].

Proper investigations of the complete wake behind vortex generators have only recently become practically possible with the advent of optical techniques such as digital Particle Image Velocimetry (PIV). Most of these studies investigate the velocity flow field behind rows of vortex generators producing co- or counter-rotating vortex cascades for certain applications. In a

* Corresponding author.

http://dx.doi.org/10.1016/j.expthermflusci.2015.10.026
0894-1777/

recent study [18] investigating snapshots of the three-component velocity field and stream-wise vorticity field behind a single rectangular vortex generator, a secondary structure was discovered which was not previously observed in studied cascade configurations (see, e.g., [19,20]). This secondary vortex has shown to be able to substantially perturb the primary vortex core itself [18] as well as its position [21,22]. Its generation was not fully understood in the setting with an oncoming stream-wise boundary layer and therefore naturally triggered the present study. Previous studies have revealed similar structures formed by local separation of the boundary layer in the lateral direction by the pressure gradient imposed by the primary vortex on the wall. Known examples include simulated aircraft trailing vortices by Harvey and Perry [23] as well as in two-dimensional computations of vortex pairs approaching a wall (see, e.g., [21]), 2D visualizations [8] and in three-dimensional flow simulations (see, e.g., [24]). Despite this prior knowledge, it is interesting to observe that none of the previous studies specific to vortex generators, at least known to the authors, report about this structure until only recently [18].

In addition, the pressure distribution closest to the wall around the leading edge of the vane in the lowest part of the boundary layer results in a horseshoe vortex system, see [22]. This is very similar to other types of junction flows around, e.g., cylinders [25], blades of axial turbines [26] and wing-body junctions [27]. These structures have also been observed and described around wedge-type vortex generators [28]. This effect was difficult to capture in the PIV measurements in the current work, since one sleeve of the horseshoe vortex was swept under the primary vortex and joined the local separation (which has the same sign of rotation) at a very early stage of the wake development. Due to problems of reflections from surfaces, such as the vortex generator trailing edge, one cannot always measure close enough to the generator to capture this vortex sleeve. Water channel visualizations could therefore aid in visualizing and confirming this anticipated effect, see [22].

The separate existence of these two types of flow mechanisms in the particular setting of vortex generator flows is now established [18,22], but the resulting far wake has not previously been studied. The present work therefore aims to extend the experimental investigation by studying the combination of these non-linear viscid flow mechanisms, showing that the resulting flow field can display a high degree of complexity as opposed to what has previously been assumed. Further, the existence of the observed viscid secondary structures and their influence on the main vortex are not previously accounted for in existing (usually inviscid) analytical models of the VG wake. This simplification can potentially yield considerable deviations of these models from the actual flow, which stresses the motivation for the current study. The focus of this study is the practically important far wake, which is displaying a steady wake topology from about 5 vortex generator heights downstream of the vane and on. The unsteady developing near wake appears only to be of minor practical interest since the performance of the vortex generator is mainly concentrated to the far wake (see, e.g., [20]). In the present work, the regimes of the far wake are therefore mapped as a function of vortex generator angle and height as well as the dependency of the circulation of the primary vortex to its proximity to the wall.

2. Experimental method

Stereoscopic Particle Image Velocimetry (SPIV) experiments were carried out in a closed-circuit wind tunnel as described in [22] and in more detail in [18]. The measurement setup is sketched in Fig. 1. The closed-loop wind tunnel, with cross section 300×600 mm, test section length 2 m and a contraction ratio of 8:1, was set to run at a free stream velocity of $U_\infty = 1.0\ \mathrm{ms}^{-1}$, corresponding to a Reynolds number $Re_\delta = U_\infty \delta/\nu = 1670$ based on the boundary layer thickness. The height of the largest vortex generator was set to the boundary layer thickness $\delta = 25$ mm at the position of the vortex generator. The wind tunnel speed was measured from the pressure drop across an orifice plate. At the inlet a turbulence generating grid with mesh size 39 mm was positioned, producing a turbulent free-stream and boundary layer. The turbulence intensity at the inlet has from LDA measurements been found to be 13% [29]. The boundary layer thickness was measured using both SPIV and laser Doppler anemometry (LDA). The time averaged streamwise velocity profile normalized by the free stream velocity measured by LDA is displayed in Fig. 2. Due to the concave shape of the velocity profile observed from the PIV measurements covering a larger wall-normal distance (not shown), the boundary layer thickness was determined by estimating the vorticity from the LDA profile, since the boundary layer can be considered the (viscid) vorticity contained part of the flow. An analogue definition could therefore be to define the boundary layer thickness as the distance over which the spanwise vorticity has been reduced to 1% of the maximum value. Since, by an order of magnitude analysis, one can discard the first term in the first vorticity component, one can estimate the spanwise vorticity satisfactorily by only the streamwise velocity and the wall-normal coordinate as also shown in Fig. 2 (see, e.g., [30]).

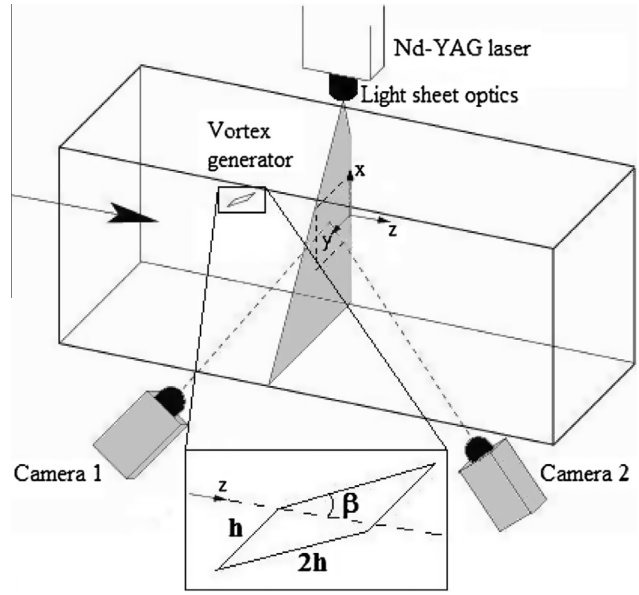

Fig. 1. Sketch of the wind tunnel measurement setup (from [18]).

The vortex generators are rectangular plates of heights $h = 5,\ 10,\ 15,\ 20$ and 25 mm and a thickness of about 0.5 mm. The vane length is always set to $l = 2h$ so that the aspect ratio is kept constant. The vortex generator was always positioned 750 mm downstream of the inlet in the center of the test section on the widest wall. A sketch of the wind tunnel test section taken from [18] is shown in Fig. 1. The coordinate system is defined in Fig. 1. z is the axial flow direction, y is the wall-normal direction and x is the spanwise direction. To accurately set the vortex generator angle, β, the vortex generator was attached to a pin which could be accessed from outside the test section through a hole in the test section wall. This pin was in turn attached to a pointer arm placed over a protractor indicating the relative angle of the actuator to the mean flow direction. The protractor had a radius of 200 mm and grading for integer values of each degree. The device angle of incidence β could therefore be set with a high accuracy.